Increase in Weather Patterns Generating Extreme Desiccation Events: Implications for Mediterranean Rocky Shore Ecosystems

Reut Zamir, Pinhas Alpert & Gil Rilov

Estuaries and Coasts
Journal of the Coastal and Estuarine Research Federation

ISSN 1559-2723

Estuaries and Coasts
DOI 10.1007/s12237-018-0408-5

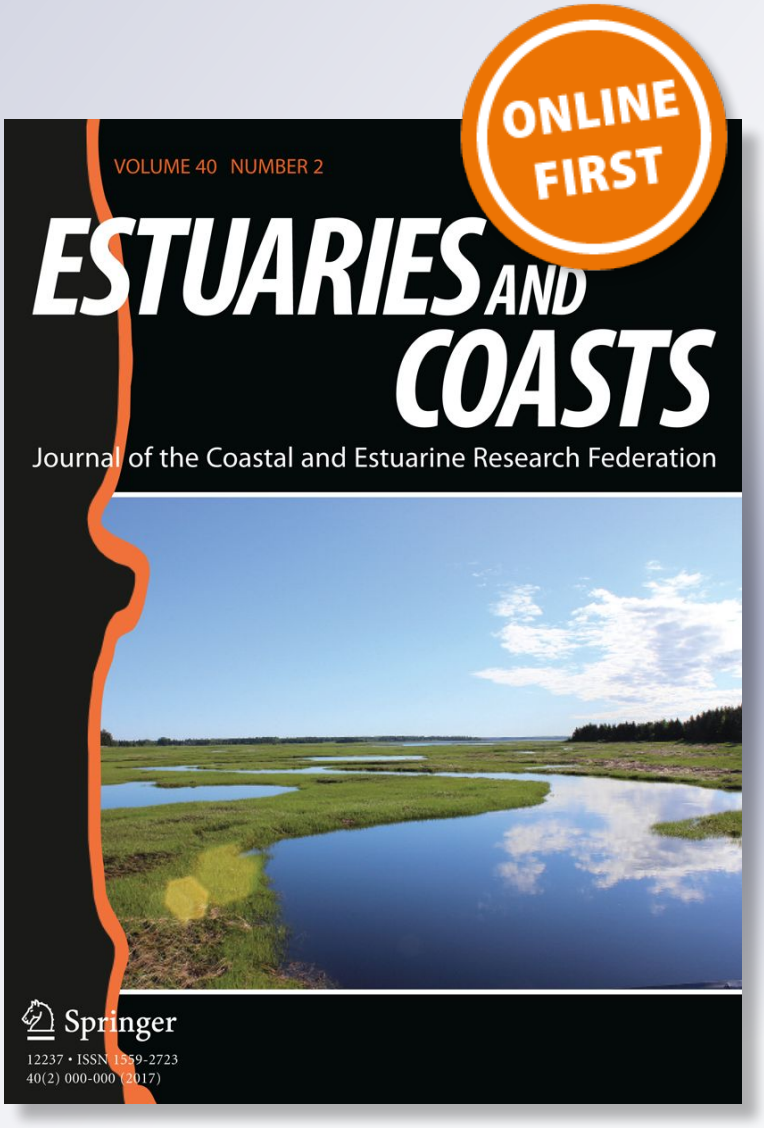

Springer

Estuaries and Coasts
https://doi.org/10.1007/s12237-018-0408-5

Increase in Weather Patterns Generating Extreme Desiccation Events: Implications for Mediterranean Rocky Shore Ecosystems

Reut Zamir[1,2] · Pinhas Alpert[3] · Gil Rilov[1]

Received: 14 August 2017 / Revised: 11 April 2018 / Accepted: 16 April 2018

Abstract

Anthropogenic global climate change is anticipated to increase the frequency and intensity of transient extreme weather events that can be catastrophic to ecological communities. Here, we characterize an extremely stressful, transient phenomenon on southeastern Mediterranean (Israel) rocky shores: prolonged desiccation events (PDE). We also examined (during 2012–2014) its potential ecological impacts on the unique intertidal Mediterranean Sea ecosystem—vermetid reefs. In this region, where the tide is minimal but the rocky intertidal is extensive, high pressure and dry easterly winds generated by specific synoptic systems can suppress tidal flooding and create stressful desiccation conditions in the lower intertidal zones for many consecutive days (several days to weeks). Very long and strong PDEs resulted in extensive macroalgal bleaching and their eventual removal from the rocks and caused mortality of stranded topshell snails and partial collapse of the mid-shore limpet population. Dominant intertidal fleshy algae were shown to be more sensitive than calcareous algae to desiccation stress, but both die after 24 h of exposure in lab conditions. Re-analysis of climatic data for the period 1960–2010 showed a considerable increase in the frequency of PDE-generating synoptic systems, mainly during winter. This means that desiccation stress has already increased on southeastern Mediterranean vermetid reef ecological communities, and if this trend continues, we can expect further increases in aerial exposure and desiccation stress that could have long-term impacts on this fragile ecosystem. These results demonstrate the importance of change in patterns of synoptic systems and wind regimes to the integrity of coastal ecological communities.

Keywords Climate change · Eastern Mediterranean · Limpets · Macroalgae · Middle East · Prolonged Desiccation Events (PDE) · Synoptic systems · Topshells · Vermetid reefs

Introduction

Anthropogenic climate change has already caused dramatic alterations to Earth's biodiversity and ecosystem functions and will continue to be a major threat for years to come (Parmesan and Yohe 2003; Gattuso et al. 2015; Molinos et al. 2015). Ongoing global change is expected not only to shift the average levels of pCO_2, temperature, pH, and precipitation by regionally variable amounts but also to increase the frequency and intensity of transient extreme events including storms and heatwaves (IPCC 2013). It has recently been suggested that increased variation, rather than changes in mean values, may represent the greater threat to species survival (Vasseur et al. 2014), stressing the need to study the effects of environmental variations and especially extreme events on ecosystems and their functions (Helmuth et al. 2014; Ummenhofer and Meehl 2017). The gradual change in mean values superimposed by particularly strong extreme events, or the cumulative effect of consecutive extreme events, may push a population or a community beyond a tipping point (an ecological threshold, Harley et al. 2017) leading to a fundamental structural and functional ecosystem shift (phase or regime shifts). The evidence of the destructive force of extreme events on marine ecosystems is starting to mount, for example, intensifying temperature extremes during El Niño

Communicated by Patricia Ramey-Balci

Electronic supplementary material The online version of this article (https://doi.org/10.1007/s12237-018-0408-5) contains supplementary material, which is available to authorized users.

✉ Gil Rilov
rilovg@ocean.org.il

[1] National Institute of Oceanography, Israel Oceanographic and Limnological Research, Haifa, Israel

[2] The Porter School of Environmental Studies, Tel-Aviv University, 69978 Tel-Aviv, Israel

[3] Department of Geophysics, Tel-Aviv University, 69978 Tel-Aviv, Israel

Published online: 01 May 2018

Southern Oscillation (ENSO) events killing coral reefs (Pala 2016) or heat waves decimating kelp forests (Wernberg et al. 2016). However, the potential increase in extreme weather events generating desiccation stress and their impacts on intertidal ecosystems have rarely been studied.

In this study, we examine the trends and potential effects of extreme events on coastal ecosystems in the Eastern Mediterranean. According to global climate models, the Mediterranean is and will continue to be one of the most affected regions by global warming and extreme climate events (Lejeusne et al. 2010), with mounting evidence of their ecological footprint on the marine biota (Marbà et al. 2015; Rivetti et al. 2014). So far though, most evidence comes from the western basin. For example, several heat waves have already caused mass mortalities of subtidal reef invertebrates in the northwestern region (Garrabou et al. 2009). The southeastern Levant (part of the Middle East) is the most environmentally extreme area in the Mediterranean region (Kitoh et al. 2008; Lelieveld et al. 2012), and signs of increase in extreme climatic conditions over the past several decades have been documented (Alpert et al. 2002; Zhang et al. 2005). The extensive climatic variability in the region makes predictions of future conditions under climate change particularly challenging, but recent regional analyses using global climate models project that on top of a temperature increase of between 3.5 and 7 °C by late twenty-first century and considerable decreases in precipitation in most Middle East areas, extreme events such as heat waves and droughts are expected to intensify, eventually becoming the norm towards the end of the century (Alpert et al. 2008; Evans 2009; Kostopoulou et al. 2013). The increase in air temperature in the region is paralleled by rapid warming of Levantine coastal waters (Sisma-Ventura et al. 2014; Ozer et al. 2016; Sisma-Ventura et al. 2014), which contributed to the collapse of sea urchin populations (Yeruham et al. 2015), and possibly many other taxa on the Israeli coast in the past few decades (Rilov 2016). Changes in wind patterns driven by climate change have not been examined in the Middle East but have been shown to cause strong impacts in several other coastal regions; for example, the intensification of coastal upwelling in eastern boundary current systems (Sydeman et al. 2014) or changes in the depth of the upper mixed layer near the Antarctic Peninsula (Montes-Hugo et al. 2009), both leading to substantial alterations in the ecology of coastal waters. Our study investigates the occurrence and potential ecological effects of prolonged desiccation stress on rocky intertidal communities on the southeastern shores of the Mediterranean in the context of apparent shifts in climate patterns, namely the frequency of specific synoptic systems that generate dry wind conditions.

The potential impacts of climate change in the rocky intertidal—an ecosystem that can be affected by change in environmental conditions in both the ocean and land—are large (Harley et al. 2006) and have been studied for more than two decades. In this ecosystem, extensive northward shifts in species distributions have been observed (Helmuth et al. 2006), and surprising latitudinal mosaics in the vulnerability of organisms to aerial exposure were also documented (Helmuth et al. 2002). Among the less-studied possible impacts of climate change on intertidal ecosystems is the potential increase in extreme intertidal desiccation events driven by changes in both temperature and wind patterns caused by shifts in the frequency and intensity of the dominating synoptic systems. In the rocky intertidal, during normal tidal cycles, species in the high tidal zone are naturally exposed to stronger and longer desiccation stress than those in the mid and low zones (e.g., Dong et al. 2008), while on wave-exposed shores, desiccation stress is normally modulated by wave splash. Prolonged aerial exposure with low humidity may result in severe tissue damage and even death in both animals and macroalgae (Petes et al. 2007; Martone et al. 2010). When the sea is calm, the risk of desiccation increases even further (Jonsson et al. 2006). On the Italian rocky shore, experimental work showed that increasing aerial exposure had negative effects both on diversity of assemblages and on percentage cover of filamentous and coarsely branched algae, but these effects were buffered by high temporal variance (Benedetti-Cecchi et al. 2006). Desiccation stress can be particularly high in intertidal areas where the tide is minimal, and dry winds frequently blow from the land seaward and can flatten the nearshore waters. Particularly long aerial exposures of the entire rocky intertidal range during seaward (easterly) winds were indeed observed on the Israeli coast where the tide is minimal (Lipkin and Safriel 1971; Rilov et al. 2004).

In the eastern Mediterranean, the tide is very small (0.2–0.4 m), but the intertidal zone can be very wide in areas where abrasion platforms, known also as vermetid reefs (Safriel 1974; Safriel 1975), dominate the shore. Vermetid reefs are unique biogenic intertidal ecosystems that in the Mediterranean are mostly found on southern shores in locations where the natural rock is relatively soft and highly erodible, and they are most extensive in the southeastern corner of the sea (Chemello and Silenzi 2011), namely Israel, Lebanon, and Syria. According to Safriel (1974, 1975), the live calcareous crust formed by vermetid gastropod aggregations protects the platforms from erosion right at sea level. The wide platforms that are formed as a result in the intertidal zone provide a rich and varied seascape that serves as habitat for a multitude of intertidal organisms (Lipkin and Safriel 1971). In the Levant basin, this habitat has been experiencing many ecological changes in the past few decades, most visibly the formation of large mussel beds of the invasive Red Sea species, *Brachidontes pharaonis* (Rilov et al. 2004), and the disappearance of the reef building vermetid, *Dendropoma petraeum* (Rilov 2016). Because the coastline in the region is straight and highly exposed to the prevailing west or northwest winds, the platforms are frequently washed by waves, especially in the summer due to continuous sea-breeze and because in this

season the tides (both low and high) are higher. This means that the ecological community on the reef flat (typically low-shore species) is mostly influenced by water temperature during the summer. However, between October and May, atmospheric conditions can generate strong, dry, easterly winds that blow over the land and seaward (Saaroni et al. 1998). These winds, when combined with high barometric pressure, can push the very nearshore water level down so that even during high tide the platforms are exposed to air (winds and pressure effectively "cancel" the expression of the high tide in the intertidal), leaving the platform exposed to dry (warm or cold) winds for long periods, sometimes days or even weeks. These prolonged desiccation events (hereafter, PDEs) have been frequently observed while monitoring biodiversity on the Israeli vermetid reefs for the past 8 years (brifely described in, Rilov 2016), and they appeared to cause massive bleaching of macroalgae and the movement or death of trapped intertidal animals.

An extensive study of easterly wind storms over Israel in the years 1983–1988 indicated that the dominant synoptic system that causes these winds is the Red Sea Trough (RST), occurring between October and May (Saaroni et al. 1998). Easterly wind storms can carry warm or cold dry air during the same season and often even during the same event (Saaroni et al. 1998). An analysis of the change in patterns of synoptic systems, conducted more than a decade ago, already showed a general trend of increase in the number of days per year under a RST system between 1962 and 2000 (Alpert et al. 2004). This may suggest that the frequency of PDE has also increased, which would result in elevated levels of desiccation stress to intertidal organisms in the past few decades.

The purpose of our study was to understand the PDE phenomenon in relation to local climate and weather, and its potential ecological impacts on intertidal communities focusing on vermetid reefs that can be highly impacted by PDEs because of their unique flat topography. Specifically, we had four main objectives: (1) to explicitly define and assess PDEs by measuring their timing, frequency, and duration and relate them to synoptic systems, temperature, and wind patterns, (2) to assess past trends of PDE-generating synoptic systems and make projections for the extent of aerial exposure for the year 2050 based on those trends, (3) to follow the fate of ecologically important compartments of the reef community during PDEs, and (4) to experimentally compare the vulnerability of key space occupiers on the rocky shore, focusing on fleshy vs. calcareous macroalgae.

Materials and Methods

Study Site

Most of the vermetid reefs in Israel are found on the north coast. Our study site was located at the Dor-HaBonim Beach where one of the longest stretches of vermetid reefs in the country is found. The site has high biological diversity and is located in a nature reserve (precluding most local human stressors). The particular study site (32° 37′ 47 N, 34° 55′ 10 E) is located on a small rocky islet, 70 m offshore, that is connected to the shoreline by a narrow rocky strip during low tide (Fig. 1). The ecological monitoring focused on two main reef zones (Fig. 1): (1) the mid-shore that has a moderate slope where the back reef meets the platform (hereafter, back reef) and (2) the low shore near the platform edge (hereafter, platform edge) where the elevated vermetid rim (Safriel 1975) absorbs most of the wave action but can be exposed during long PDEs. In between is the wide platform center, which normally holds water during low tide and calm seas but can also dry completely during particularly long PDEs. The seaward edge has the highest species diversity on the reef (Herut 2016).

Focal Functional Groups and Organisms

Our study focused on two dominant functional groups: macroalgae and grazing gastropods. We followed fleshy and calcareous algae (that may have different vulnerability to aerial exposure) near the platform edge over the study period. For the aerial exposure experiment (see below), we selected two dominant red algae species: the fleshy articulated *Laurencia papillosa* and the calcareous articulated *Jania rubens*. We focused on the two most abundant gastropod taxa in the back reef mid-shore level: topshells (*Phorcus turbinatus*) and limpets (Lipkin and Safriel 1971). In this region today, there are two main species of limpets that are difficult to tell apart without removal and therefore were not distinguished in this study: the native *Patella caerulea* and the invasive IndoPacific *Cellana rota*. Limpets strongly attach to rocks with vacuum and mucus and move slowly, mostly at night to avoid desiccation stress. *P. caerulea* have a homing behavior, returning back to its "home scar" after foraging (Williams et al. 1999). Not much is known on the biology of *C. rota*, but other members of the genus *Cellana* are not know to have a homing behavior (e.g., Williams and Morritt 1995). *Topshells* are much more mobile and can usually avoid desiccation by quickly moving to shaded, moist micro-niches, or down towards the water during low tide (Prendergast et al. 2013) or PDEs.

Identifying and Monitoring PDE

Identifying and quantitatively documenting the occurrence of PDEs in the rocky intertidal (without the need to be in the field to observe it) are not trivial tasks. The best way to identify a PDE is to know when the reef flat (low shore) remains exposed to air during high tide, i.e., when nearshore waters are depressed below the reef flat level. We define a PDE as

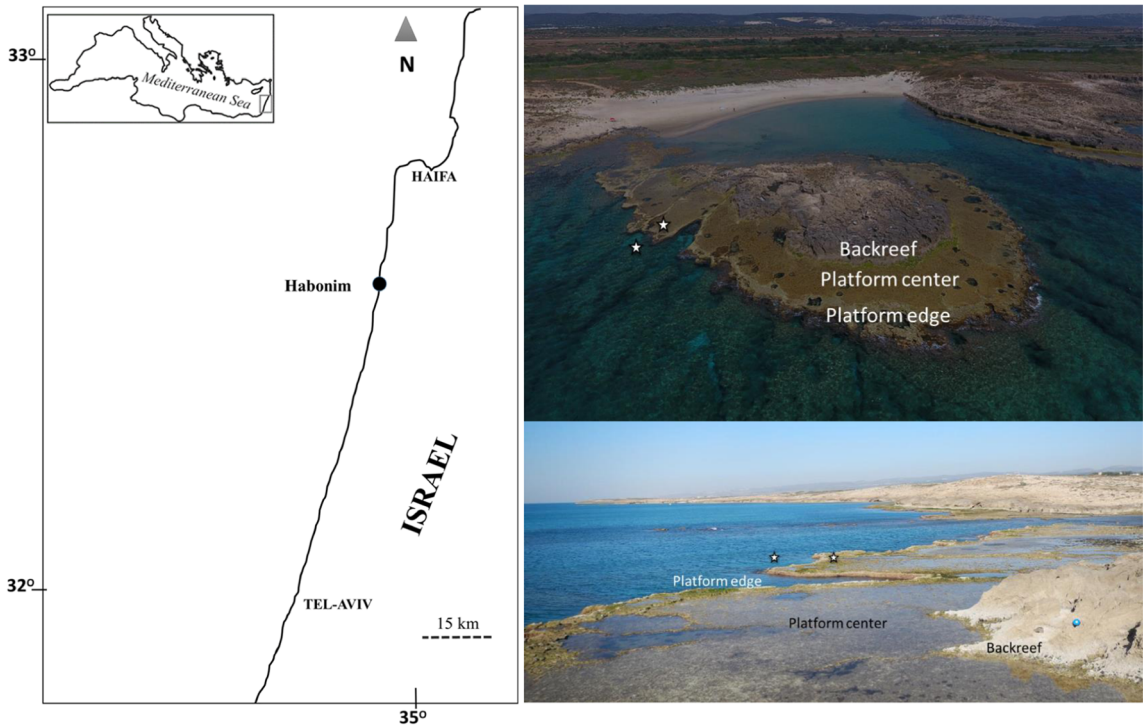

Fig. 1 Location of the main study site, Habonim, on the Israeli coast, and a drone photo and a side view of the HaBonim study site. The different zones are indicated as well as the location of the intertidal and shallow subtidal temperature loggers (stars)

including at least two consecutive high tides during which the reef flat is exposed to air. Two main types of physical measurements can be used to inform whether the rock surface is out of the water: a pressure sensor that measures water level above the rock (Mislan et al. 2011), or temperature sensors (Harley and Helmuth 2003) that can be used to compare the temperature differences between the low shore level and the shallow subtidal waters, or to the air temperature measured in the region (above the intertidal zone). We used the temperature comparison method. If low shore (platform flat) temperatures and shallow subtidal temperatures are identical for a period of time, it almost always means that the reef flat is covered by water and washed by the tide and/or waves. If they are different (higher or lower), it means that the reef flat is exposed to air and influenced by air temperature which normally varies more than water over short time scales. Similarly, if temperature measured in the low shore level and the regional air temperature are similar and synchronized, it also would normally mean that the platform is exposed to air. Temperatures in HaBonim were measured with TidBiT v2 data loggers (Onset Computer Corporation) that recorded temperature hourly, one installed (hanging inside a protective cage) on the platform flat behind the edge (low shore level) and the other on a rock surface, about 5 m away, at a depth of 0.5 m (shallow subtidal, always underwater, Fig. 1). Regional air temperature data were taken from the Israel Meteorological Service Coastal Weather Station in Hadera, about 15 km south of HaBonim. We used local temperature and weather data measured over 4 years (March 2010–May 2014) to understand the relationship between PDEs and the physical conditions in the area. For most of the 4 years, we used the difference between platform and water temperature as the proxy for aerial exposure, but between February 15 and October 30, 2012, the water logger malfunctioned and we used instead the platform and air temperature similarity as the proxy.

We determined a difference of 1.5 °C or more between the platform and water loggers as the threshold indicating aerial exposure, considerably more than the accuracy of the instrument, ± 0.2 °C, to minimize potential false positives. For the platform to air temperature comparison, the threshold was a difference < 1 °C, indicating aerial exposure. The temperature difference method will sometimes under-represent the occurrence or length of a PDE period as it will not take into account PDE times when air and water temperature are very close. In a few cases, we decided to use additional metrics to determine that the reef was most probably exposed to air even though the temperature data did not conform to the stated thresholds. For example, we considered a time step in the data as exposed to air even if the temperature difference between the platform and water was slightly smaller than 1.5°, but only when the platform temperature was similar to air temperature and this time step was a small gap in what appeared to be a long, continuous, PDE. During the period when only air and platform temperature data were available, we also considered the platform as exposed to air even if platform and weather station air temperature was different in the winter months when

temperatures measured on the platform were well below the expected water temperature for the season (for example, 5 °C in March when water temperature should vary between 15 and 18 °C based on data from other years). This is because air temperature in the winter very close to the surface can be considerably cooler than that measured in a weather station a few meters above the ground.

Temperature data used for PDE analysis were based on measurements taken between March 9, 2010 and May 16, 2014. For that period, tide level was determined from the predicted sea level data for the Israeli shore provided by Israel Oceanographic and Limnological Research (IOLR) or from the Survey of Israel Center. We also aimed to determine what percentage of the platform's aerial exposure was driven solely by PDE-generating weather conditions (winds and/or barometric pressure and not low tide). For that, we needed to align the temperature records with the predicted tide record and taking into account the height of the platform. Only times when the high tide level was high enough to cover the platform but the temperature records indicated aerial exposure of the platform were considered as exposure solely driven by the local weather conditions. The average height of the reef flat at HaBonim is 22 cm above mean sea level. It was measured with a laser level (Trimble Spectra Precision Laser) relative to a benchmark with a known absolute elevation. We also aligned the temperature with wind and humidity data obtained from the Hadera weather station. A PDE was considered as at least 9 h of exposure (analysis was done on temperature data in 3-h intervals), i.e., including at least two consecutive aerial exposures during high tide with one low tide in between. Aerial exposure trends were based on four main metrics: (1) the number of aerial exposure events, (2) the average and (3) maximum length of the exposure, and (4) the exposure hours generated by each synoptic system per season.

Assessing Past, Present, and Future Trends in PDE-Generating Synoptic Systems

To understand the relationships between PDEs, local weather conditions, and atmospheric synoptic systems, we focused on the data collected for the period mentioned above. For this period, we calculated correlations between PDE occurrences identified by the temperature difference data measured in HaBonim, and the weather data measured during those occurrences by the weather station (wind direction and speed, humidity) as well as the type of synoptic system that dominated during every documented PDE. Wind direction was calculated following Grange (2014), where the direction was separated to its U and V components in radians, and calculated considering wind speed since the vectors are weighted by their magnitude. The average of each component was calculated, and then, by using arctan function, the two components were averaged to give final mean wind direction.

In order to understand in more detail the climatic characteristics during PDEs, assign a specific synoptic system to a specific PDE or non-PDE period, and update the temporal patterns in the dominant synoptic systems that generate them, we have used a model that was developed to automatically identify the typical synoptic systems that occur in Israel (Osetinsky 2006). Osetinsky's study used five synoptic systems that are divided into 19 different types classified for the Middle East in a previous work (Alpert et al. 2004) to investigate regional climate trends and their connections with global trends and for the development of regional climate simulations using global/regional circulation models (GCM/RCM). Further, we used Crosstab analysis (SPSS software) in order to find for each synoptic system, in which season it had the most effect during a PDE, that is, when it had the highest frequency compared to the other seasons. Then, based on this information, we performed reanalysis of the synoptic system data of the past 40 years to search for possible changes in the frequency of occurrence of systems that were found to correlate with long PDEs (e.g., the RST). For systems showing a substantial change in one season or more over the past 40 years, we projected the change in PDE occurrence (in terms of cumulative aerial exposure hours per season) for the year 2050, by assuming that the past trends (based on simple linear regression) will continue over the next few decades. We calculated the average number of exposure hours in a single event in the last 4 years and multiplied it by the percentage of expected change in the occurrence for the system responsible for the event by year 2050, to forecast the change in exposure hours for that year for each season. The seasonal distribution was predetermined and is as follows: spring: March–May, summer: June–August, fall: September–November, winter: December–February (Council 2001).

Ecological Monitoring During PDEs

In order to track the dynamics of several important functional groups of the vermetid reef that might be differently affected by PDEs, we performed nearly weekly monitoring of the rock cover of major macroalgae functional groups at the platform edge, as well as the density of gastropod grazers at the back of the reef. For that, a 50-m transect tape was laid along the platform edge or back reef, and in 15 random locations along the tape, the macroalgae cover (edge) or gastropod density (back) were monitored inside a 0.5×0.5-m quadrat divided into 100 subquadrats. Monitoring at the reef edge was conducted between September 2012 and June 2014 and at the back reef between September 2013 and June 2014. We also conducted intense monitoring in five permanent quadrats (corners fixed with stemless steel bolts) between November 2013–June 2014 that was added to allow a closer look of the change in the dominant macroalgae taxa specifically before, during, and after a long

and intense sets of events that started in mid-December 2013 and were monitored almost on a daily basis for the first 2 weeks and more sparsely afterwards.

Testing Algal Sensitivity to Desiccation

We decided to focus our lab experiment on sessile low-shore organisms as we assume that they are the ones that would be firstly affected by prolonged desiccation (they cannot move or hide). *J. rubens* and *L. papillosa* were selected for our experiment, because they are important space occupiers near the edge of the reef for at least part of the year, and previous field observations suggested that they have different sensitivities to desiccation (Rilov personal observations). To test their vulnerability to desiccation, 18 intact thalli of each species at a size of about 3 cm were removed from the reef on October 5 2014 and brought to the lab at IOLR. Each specimen was measured, weighed (wet weight after drying with a paper towel), and placed in a Petri dish. Petri dishes were placed in an outdoor 1-m^3 plastic tank filled with a thin layer (2 cm) of running seawater (supplied from 1-m depth) to simulate intertidal conditions when the platform is gently washed by water. After an acclimation period of 1 week, we exposed the algae to five different durations of aerial exposure, with three replicates per treatment. The exposure treatment durations were 6, 12, 24, 48, and 72 h. We measured the performance of the algae at three time steps: just before the beginning of the aerial exposure, immediately after the end of the exposure period, and after 24 h in running seawater to test for possible recovery of the algae. The control (not exposed to air) treatment included three algae that were submerged in a Petri dish during the entire experiment. Their photosynthesis rates were measured at the beginning of the experiment, after 72 h, and again after 24 more hours in parallel to all other treatments. Skies were clear during the 4 days of the experiment and all measurements were taken at 12:00 PM and therefore light conditions were similar. We used net photosynthesis (measured as the amount of net dissolved oxygen produced per gram wet weight) to assess the performance (state) of the algae underwater. Measurements were conducted by incubation of each specimen in a 1-l sealed glass jar for 1 h and measuring the oxygen concentration in the water before and after the incubation with an optic sensor (WTW ProfLine Oxi 3310).

Results

PDE Trends and Aerial Exposure

During the 4 years of the studied period, there were 169 PDE occurrences in HaBonim and most of them occurred between late October and mid-May (Fig. 2), resulting in 1530 h of reef platform aerial exposure (average of 16 days per year). However, PDE frequencies and durations varied greatly over the 4 years. In 2012, PDEs occurred in high frequency and extended their duration starting in early April and ending in mid-June; that is, spring PDE generating conditions stretched until mid-June (June in our analysis was considered summer). Between mid-December 2013 and the end of January 2014 easterly winds, mostly cold, dominated the weather, resulting in multiple, almost continuous, PDEs with only occasional, short, platform immersion periods. The relative frequency of different exposure hours is shown in Fig. 2b. Figure 3 shows different parameters per month: number of aerial exposure events, number of PDEs, maximum continuous exposure, and average exposure duration during PDE. Extreme PDEs at the 90th percentile lasted longer than 20 h, and PDEs that lasted more than 36 h of aerial exposure were at the 95th percentile, which occurred 22 times during the 4 years of the study. Exposures longer than 100 h occurred only three times during that period (the 99th percentile, Fig. 2b). The longest continuous PDEs lasted 141 h, i.e., almost 6 days, and occurred in March and December 2011, and the third longest, 120 h, occurred in December 2013 (Fig. 3).

Table 1 presents PDE statistics per season. Winter and spring had the highest number of PDEs, and the greatest contribution of climate to the events was during fall and winter (over 50%). PDEs were associated with easterly winds (mostly northeasterly) more than 50% of the time (Fig. 2c), and the rest of the PDEs occurred when weak westerly winds occurred (i.e., calm sea conditions). The strongest winds (12–14 m/s) came directly from the east (Fig. 2c).

The median temperature on the reef during PDEs in the transition seasons (Fig. S1 in Appendix 1 of the Supplementary information), fall and spring, was very similar (20 °C), but the range was larger in the spring. Temperatures were lower during winter PDEs (13 °C), and they ranged widely from close to 5 to near 30 °C. During summer, the average PDE temperature was highest (23 °C). Climate contribution had different effects on the reef in each season. Following, are the dominating synoptic patterns producing PDEs by season (see system categories and their numerical coding in Appendix 2).

Spring Synoptic Patterns (March–May)

About 46% of the PDEs occurred during the spring season (Figs. 3 and 4). The High to the West (H_W) and the Red Sea Trough with an Eastern axis (RST_E) were responsible for the greatest number of accumulated exposure hours, when mostly easterly winds were blowing (Fig. 4). The H_W system also dominated the atmospheric conditions during the longest exposure period in this season (6 days). During these PDEs,

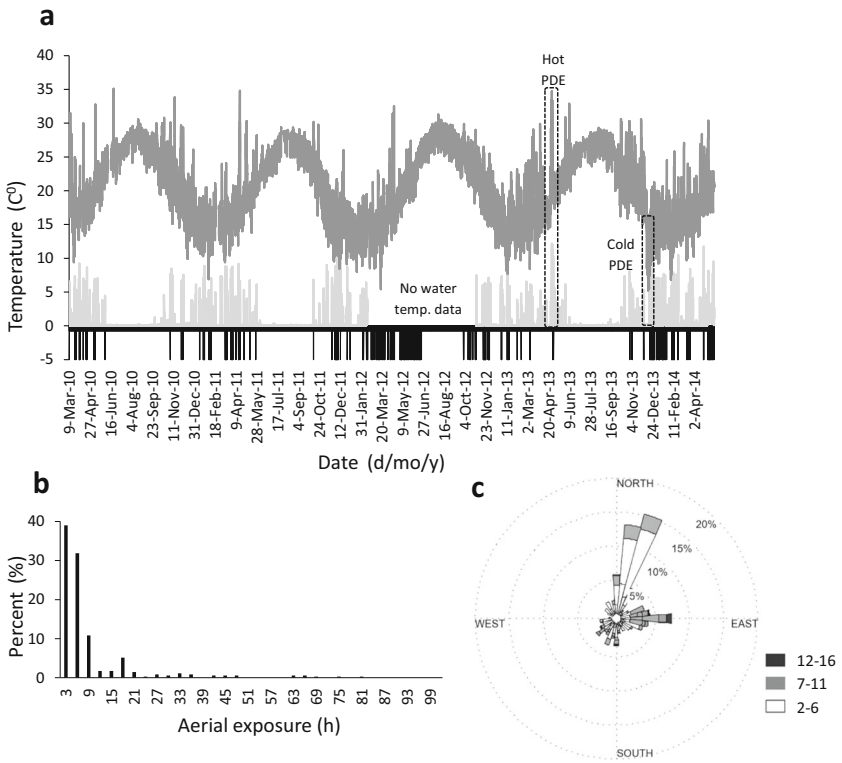

Fig. 2 Physical conditions during PDE and the low intertidal aerial exposure trends between March 2010 and mid-May 2014 in HaBonim. **a** Air temperature (dark gray), absolute temperature differences between platform logger and shallow water logger (light gray), and aerial exposure occurrences based on temperature differences (shown as vertical lines below the zero line). Examples of hot (in spring) and cold (in winter) PDEs are shown in boxes. **b** Relative frequency (in percentage) of different aerial exposure durations during the studied period. **c** Frequencies of wind direction and speed (above 2 m/s) that occurred during PDEs throughout the entire research period. The shading refers to the wind speed, and the percentage refers to frequencies of events in a specific direction. Fifty-seven percent of the exposure events were under the effect of eastern winds above 2 m/s

temperatures were significantly higher than outside PDE periods, and wind direction was significantly dominated by easterlies (mean wind direction was 118°, Table 2, Fig. 3). The other synoptic systems that occurred during PDEs were High to the North (H_N), High Over Israel (H_C), and the Cyprus Low to the North (CL_N-S).

Summer Synoptic Patterns (June–August)

The most frequent synoptic systems during summer PDEs were the Persian Trough Weak (PT-W), the Persian Trough Medium (PT-M), and the High to the West (H_W). These systems were also responsible for most of the exposure hours, and the H_W was responsible for the longest exposure in the season (more than 3 days in summer 2012). During these PDEs, there were relatively lower temperatures for the season, but wind direction or speed did not significantly differ between PDE and non-PDE periods (Table 2).

Fall Synoptic Patterns (September–November)

The most frequent synoptic system during fall PDEs was the Low to the East Shallow system (L_E-S), but RST_E and H_W were responsible for most of the exposure hours (Fig. 3). The RST_E caused the longest exposure (+ 3 days). During fall PDEs, winds were significantly stronger but wind direction or air temperature did not significantly differ between PDE and non-PDE periods (Table 2).

Winter Synoptic Patterns (December–February)

The most frequent synoptic systems during winter PDEs were RST_E, RST_C, and H_N. These are also responsible for most of the exposure hours, but the longest exposure occurred during H_E and H_W that are not frequent during this season. During PDEs in winter, temperature, wind speed, and direction significantly differed from non-PDE periods (Table 2) as PDEs had a colder easterly flow.

Synoptic Trends Between 1960 and 2010 and Predictions for 2050

A significant increase in frequency of the synoptic systems dominant during PDEs was found between 1960 and 2010 for both the summer and winter seasons. The PT-W—the

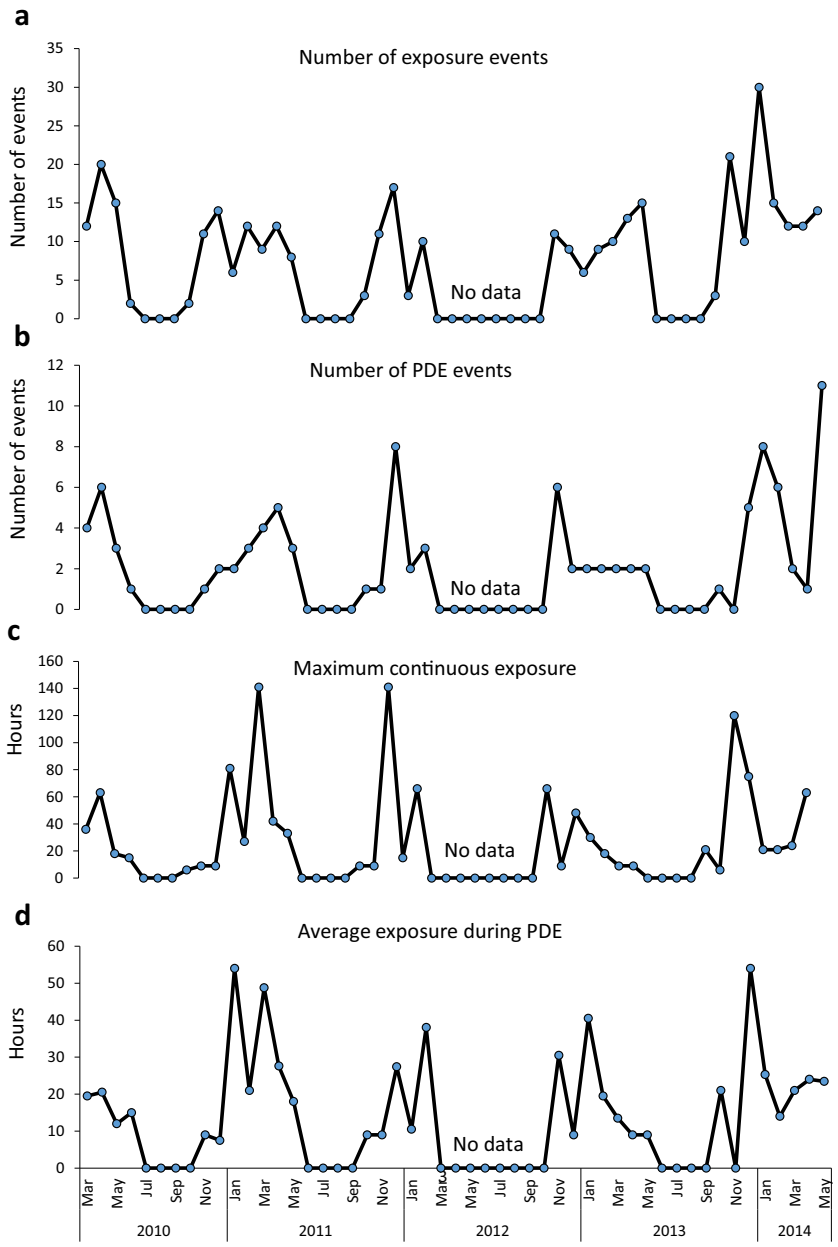

Fig. 3 Monthly averages of the number of all aerial exposure events (**a**), number of PDE events (exposures ≥ 9 h) (**b**), maximum continuous exposure (in hours) (**c**), and average exposure hours during PDE (**d**) (pay attention for different *Y*-axis scales)

system responsible for the longest PDE in summer season in 2012—showed an increase in frequency, mostly since the early 1990s (Fig. 5). If this trend will continue linearly in the future, then by 2050, the average number of exposure hours in that season will increase from 15 today (based on the 2010–2014 data) to nearly 24 h (Fig. 5). The synoptic systems that were producing the most intense PDEs in the winter, the RST eastern and central axis (RST_E, RST_C), also showed a significant increase in frequency (Fig. 5), with more than doubling in frequency after 1990 compared to the period 1960–90. If the increasing trend of those systems is maintained, then by 2050, the predicted aerial exposure hours during winter will more than double again (each system will add approximately 38 h, Fig. 5).

Temporal Dynamics of Dominant Functional Groups during PDEs

Of the 60 weeks between February 2013 and May 2014, we sampled the platform edge community on 28 occasions. During the summer, sampling was almost impossible due to the constant wave action on the platform generated by the daily sea breeze, and in winter, there were several weeks when sea conditions were too rough to sample.

Macroalgae

At the reef edge, the calcareous and non-calcareous (fleshy) algae showed an opposite temporal trend in rock cover

Table 1 Prolonged desiccation events (PDEs) statistics by season calculated over a period of 4 years. For each season, we show the average number of PDEs, their average duration in hours (plus standard deviation, SD), the average duration of PDE contributed only by atmospheric contribution to the event (total exposure hours minus exposure hours that occurred during the predicted low tide), and the total seasonal atmospheric contribution to PDE occurrence in percentage out of averaged exposure hours. EPP = exposure per PDE, AC = atmospheric contribution, SAC = seasonal atmospheric contribution. Corresponding months for each season were as follows: spring: March–May, summer: June–August, fall: September–November, winter: December–February

Season	Total no. of PDEs	EPP (h)		AC (h)		SAC (%)
		Average	SD	Average	SD	
Spring	84	16.4	4.68	7.08	2.67	43.1
Summer	11	24.8	5.50	9.00	2.24	36.3
Fall	22	19.1	5.86	10.77	5.59	56.4
Winter	52	21.5	5.48	12.33	5.48	57.3

(Fig. 6a) resulting in a strong negative correlation ($r = -0.87$). During winter and spring of 2013, calcareous algae (mostly *J. rubens*), which initially dominated, reduced in cover while fleshy algae (mostly *Laurencia* and *Ulva*) increased (Fig. 6b), leading to a switch in dominance by late spring. The decrease of fleshy algae in June followed a short but very warm PDE in late May (air temperatures above 30 °C, indicated by a rectangle in Fig. 2, and by a black arrow in Fig. 6a). By contrast, fleshy algal dominance in early winter reduced considerably from late December to spring 2014 (almost zero in late April), during and following the longest PDE sequence in the study period (indicated by a rectangle in Fig. 2 and arrows in Fig. 6a, see below) when dominance switched again towards calcareous algae; however, these calcareous algae (mostly *J. rubens*) were bleached during most of that period (Fig. 6b). Some recovery of fleshy algae (but mostly ephemeral, opportunistic, taxa from the family Ulvaceae) was seen in early May 2014 (Fig. 6a, b). We observed that during short PDEs (9–48 h), bleaching in dense algae mats only appeared at the tips of the algae, which later presumably break off the plant leaving below mostly health thallus (normal color), resulting in a quick recovery of the local population. Under long PDEs and especially following strong easterly winds that dry the platform completely (like in the series of PDEs in winter 2013–14), the whole thallus bleaches and dries and eventually crumbles. Over time, when strong waves wash the platform, most of the algal biomass is washed away, leaving mostly bare rock or bleached encrusting algae behind, and the vacant space is quickly taken over by spring ephemeral fleshy algae.

Grazing Gastropods

Over the 9 months of mobile grazer monitoring, the topshell *P. turbinatus* at the back reef showed high variability in density with no clear temporal pattern (Fig. 6b). The limpet density initially increased in abundance until mid-September 2013, then decreased in late September, and sharply dropped again in late December following exposure to very high (31 °C in early December) and then cold air (7–10 °C in mid-December) during the early stages of the long PDE sequence that started in mid-December 2013. Limpet density remained very low for the rest of the study period.

As mentioned above, the longest sequence of PDE events started on 14 December 2013 and was characterized (mostly) by cold and dry easterly winds (textual and pictorial depiction of the sequence of events are shown in Online Resource, Appendix 3). On December 16, minor bleaching was visible at the edge of the platform on the elevated rim but most of the reef area still appeared healthy because the platform center still held water, but there was no flushing. On December 17, the platform center began drying and the algae there began to bleach, while the back reef topshells moved lower and aggregated in wet pits and crevices (micro-refugia). By December 26, the whole platform was bleached, and many dead topshells were seen in by then fully dried "refugia". Limpet mortality was also observed. We also observed the mortality of other animal species trapped in shallow tidepools where water levels reduced. These included crabs, sea cucumbers, other snails, and tube worms.

Algal Sensitivity to Desiccation: Fleshy vs. Calcareous Macroalgae Vulnerability Experiment

In *L. papillosa*, clear signs of bleaching were already seen after 6 h of aerial exposure, photosynthetic activity in water reduced substantially, and there were no signs of recovery after 24 h in running seawater (Fig. 7), indicating that the specimens were dead after 6 h in air. Bleaching was more severe during longer exposures and dissolved oxygen (DO) values were negative, indicating net respiration, probably by bacteria on the decaying algae. In *J. rubens*, after 6 h of aerial exposure, DO values have increased by 25%, indicating increased photosynthetic activity, but DO reduced following longer exposures. After 24 h in running seawater, photosynthesis in specimens exposed to air for 12 and 24 h had improved, but there was no recovery in specimens exposed for 48 h or more, indicating that they did not survive these long aerial exposures.

Discussion

This study is the first to investigate the relationship between climate patterns (synoptic systems), shoreline weather patterns, and extreme desiccation conditions in the coastal environment. We demonstrate that prolonged desiccation stress (from many hours to days) is a frequent phenomenon in the mid- and low shore zones of vermetid reefs, a unique and

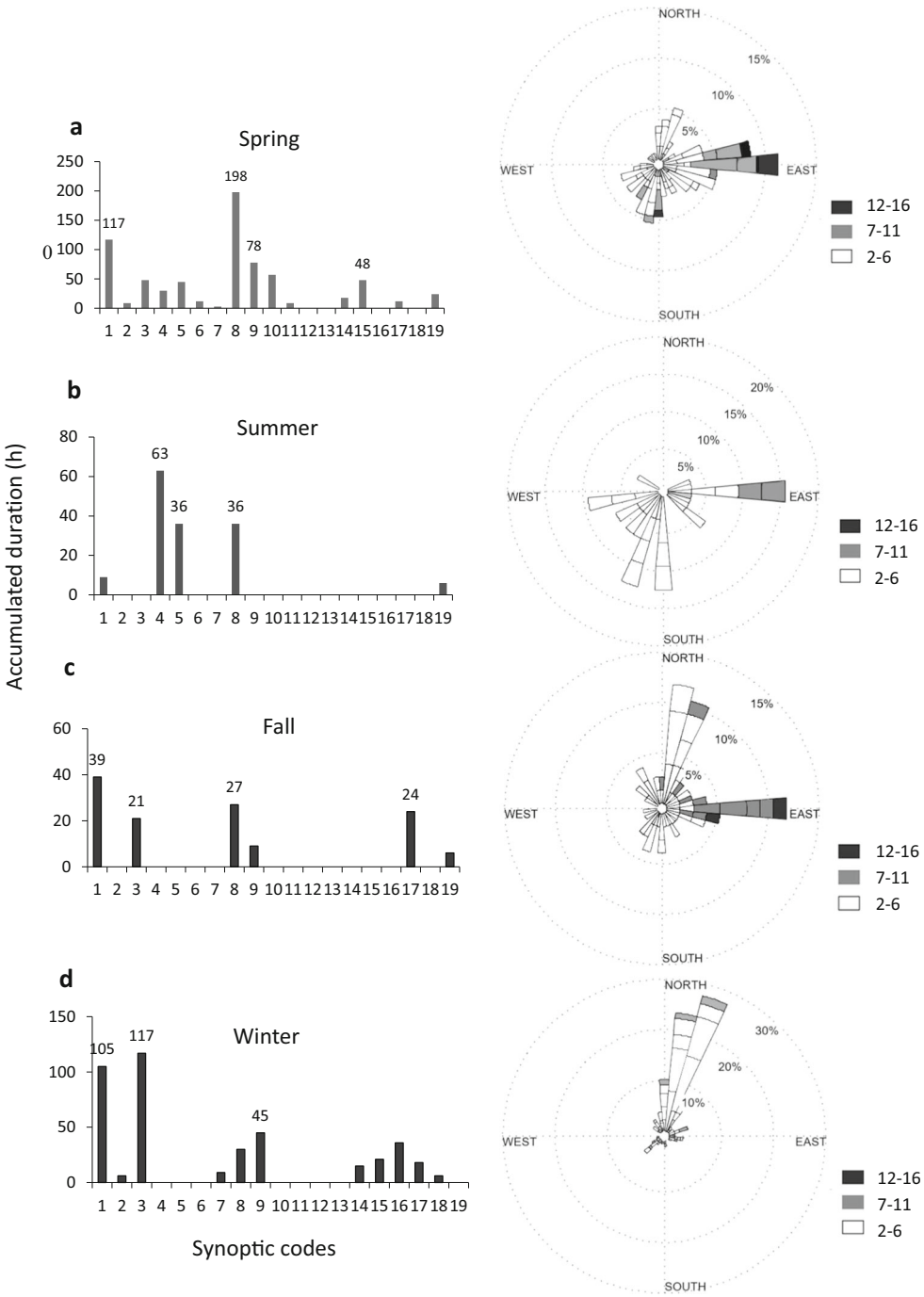

Fig. 4 Accumulated hours of aerial exposure during high tide under the influence of all the synoptic systems (4 years) and wind roses showing the dominating winds (speed and direction) during PDEs for the spring (**a**), summer (**b**), fall (**c**), and winter (**d**) seasons. The synoptic code index is found in the Online Resources (Appendix 2). See Fig. 2 for explanation on the windrose data

fragile rocky intertidal ecosystem on southeastern Levant shores. The most extreme events (at the 90th and 95th percentiles) can last more than 20 and 36 h, respectively, and occasionally (< 1% of the aerial exposure events) up to 6 days of continuous exposure to hot or cold dry air. The most extreme PDEs cause massive bleaching of algae (and the eventual removal of all erect algal biomass, fleshy or calcareous), considerable mortality of mobile gastropod grazers that are trapped on the platform, as well as other animals. We have shown that two dominant algal species have different sensitivities to desiccation stress, but long PDEs eventually kill all algae. We have also identified the synoptic systems that are responsible for most PDEs, and using reanalysis of weather conditions, we detected considerable increases (by two fold or more) in the frequency of occurrences of these systems in summer and more importantly in the winter months, the

Table 2 Comparison (*T* test) of air temperature (AIR TEMP), wind speed (WIND SP), and direction (WIND DIR) ($p < 0.05$) between non-PDE and PDE periods (reef exposed during high tide). Significant differences are marked in bold. * Mean wind direction and SD were calculated by averaging the vector direction (see text for explanation). Corresponding months for each season were as follows: spring: March–May, summer: June–August, fall: September–November, winter: December–February

Parameter	Period	*N*	Mean	SD	SE	*p*
Spring						
AIR TEMP	Non-PDE	3271	18.87	3.29	0.05	**< 0.001**
	PDE	236	19.71	3.31	0.21	
WIND SP	Non-PDE	3271	4.23	2.49	0.04	0.697
	PDE	236	4.16	2.72	0.17	
WIND DIR	Non-PDE	3271	310*	93*	1.90	**0.014**
	PDE	236	118*	70*	9.22	
Summer						
Parameter	Period	*N*	Mean	SD	SE	*p*
AIR TEMP	Non-PDE	2742	26.55	1.98	0.03	**0.003**
	PDE	50	25.71	2.16	0.3	
WIND SP	Non-PDE	2852	3.79	1.46	0.02	0.917
	PDE	50	3.82	1.64	0.23	
WIND DIR	Non-PDE	2852	264*	64*	1.27	0.902
	PDE	50	171*	104*	12.15	
Fall						
Parameter	Period	*N*	Mean	SD	SE	*p*
AIR TEMP	Non-PDE	2821	23.59	3.75	0.07	0.562
	PDE	88	23.82	4.91	0.52	
WIND SP	Non-PDE	2824	3.87	2.27	0.04	**0.010**
	PDE	88	4.51	2.21	0.23	
WIND DIR	Non-PDE	2824	347*	56*	2.07	0.105
	PDE	88	16*	72*	13.82	
Winter						
Parameter	Period	*N*	Mean	SD	SE	*p*
AIR TEMP	Non-PDE	2675	15.41	3.15	0.06	**0.040**
	PDE	136	14.84	2.83	0.24	
WIND SP	Non-PDE	2729	4.47	2.62	0.05	**0.030**
	PDE	136	4.06	2.04	0.17	
WIND DIR	Non-PDE	2729	173*	89*	1.74	**< 0.001**
	PDE	136	72*	6.5*	4.53	

growth season of most algae, and the season with the highest biodiversity on Levant vermetid reefs (Rilov, unpublished data). So far, research that focused on changes in dry (desiccating) conditions associated with anthropogenic climate change has only discussed it in the context of increase in drought intensity and frequency on land, in both the Middle East and globally (Diffenbaugh and Field 2013; Kostopoulou et al. 2013; Kelley et al. 2015; Mann and Gleick 2015; Tielbörger et al. 2014); a change that can have huge ramifications to both natural and agricultural terrestrial ecosystems (IPCC 2012), e.g., desertification (Romm 2011) and loss of crops (Lesk et al. 2016). Although more research is needed on both the climatological and ecological aspects of the PDE phenomenon, described here for the first time, our results present evidence for a recent increase in atmospheric conditions in the Middle East that produce extreme stress to intertidal ecosystems. The field and lab results, though limited in spatial expanse, duration, and scope, indeed demonstrate the severe ramifications that increased PDEs can have on rocky intertidal ecosystems in the region.

PDE Characterization and Patterns

Aerial exposure periods that are driven solely by atmospheric (synoptic systems) and local weather conditions (mostly easterly winds), i.e., not by low tide, were successfully identified using the temperature difference method. That said, this method will not identify specific times when the lower intertidal is exposed to air during high tide, while air and water temperatures are very similar. Likewise, at times when air, platform, and water temperatures are very similar (we assume that such occurrences are rather rare and are mostly expected in the summer), there can be false negatives or positives if only platform and air temperature are used. In our study, to reduce those potential false negatives and positives, we looked at the temperature data before and after such occurrences as well as the wind and tide data and used our expert judgment to decide if the platform was exposed to air. The use of accurate water level pressure sensors on the platform surface may overcome this ambiguity. More than 50% of aerial exposure hours could be directly explained by atmospheric contribution (i.e., not by low tide) during winter and fall. This means that most of the PDEs in those seasons can be predicted by weather forecasts. Especially surprising were the results for winter when stormy conditions (and thus wave action) are prevalent. The atmospheric contribution to aerial exposure was lower in spring (43%) and especially in the summer (36%) when strong sea breeze generate waves that wash over the reefs almost constantly, also during low tides.

The highest frequency of PDEs took place in the spring (mostly short ones). This is a result of the unstable weather that characterizes transitional seasons which includes the widest range of synoptic systems that pass through the southeastern Levant region. The longest PDEs occurred once in the spring and twice in the early winter months. The prominent systems forming PDEs were indeed characterized by easterly winds that caused prolonged, very dry, aerial exposure (sometimes for many days) by pushing the very nearshore seawater levels down, preventing the expression of high tide on the reef flat.

The considerable increase in frequency of PDE-generating systems (mainly RST during winter) over the past 40 years could have significant ecological consequences. The increase in frequency of RST was not steady but rather showed a major

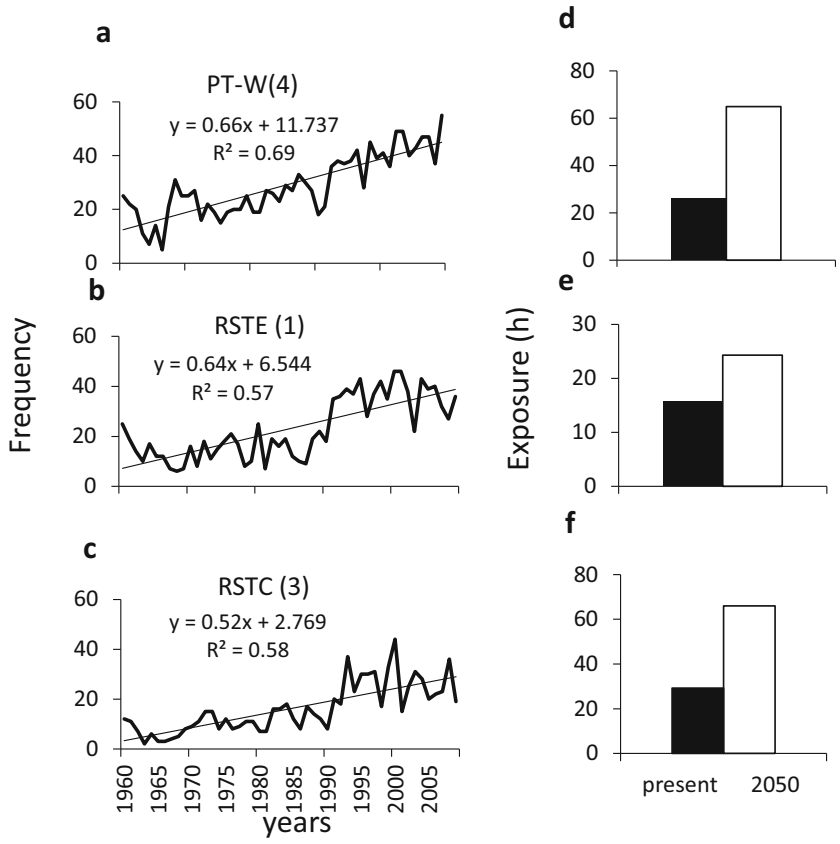

Fig. 5 The frequency of the occurrence of synoptic systems 4, 1, and 3 between 1960 and 2010 (**a**, **b**, **c**) and the present (calculated from the field data for 2010–14) and projected hours of aerial exposure in 2050 based on the equation of the linear regression in **a**, **b**, or **c** (**d**, **e**, **f**)

shift (more than doubling) during the early 1990s. Signs of this increase in the 1990s were already suggested in an earlier study that analyzed this synoptic system's trends until 2000 (Alpert et al. 2004), and our data show that in the last decade, those much higher RST frequencies persist, although inter-annual variations are considerable. In parallel, analysis of flooding trends in the Israeli Negev desert has shown increase in flood events associated with the RST over the past 40 years (Shentsis et al. 2012), which can likewise have significant ecological impacts on desert ecosystems. This dominant PDE-forming system is more typical to transition seasons and thus, its dramatic increase in frequency in the winter may suggest a shift in seasonal timing and characteristics: winter becoming more similar to spring in the Middle East. Such climate change-related shifts have already led to considerable phenological shifts in different ecosystems globally (Visser and Both 2005). The increase in frequency of PDE-generating systems, especially during winter, means that desiccation stress has already increased on vermetid ecological communities in the Middle East over the past few decades. If the trend continues, our rough estimations project a doubling in exposure hours during winter by 2050. The longest sequence of PDEs took place in the winter of 2013–14 and initiated in mid-December with a H_W system that started with very cold easterlies that were followed by warm and dry southeasterly flow. Following exceptionally high temperatures for December (over 30 °C) where 6 days of continuous aerial exposure with temperatures dropping on the platform at night below 8 °C. It was then alleviated by 2 days of submergence and then continued with several shorter PDE intervals until late January 2014, concluding almost a month and a half of highly stressful conditions at the main growing and most diverse season of intertidal macroalgae in the region.

There was only one long PDE (3 days) over the 4 studied years that occurred between June and September (all of summer and early fall). It started at the beginning of summer 2012 (June 4) when a Persian Trough system prevailed, which is characterized by weak westerly winds. This unusual occurrence can be again a result of changes in the seasonal timing where spring climate conditions extend into the normally summer months. Indeed, the reanalysis showed that the Persian Trough steadily increased its frequency over the past 40 years. This system carries the highest air temperatures, compared to the other summer systems. If indeed this system will continue to intensify on the expense of other summer systems, we should expect increasingly warmer summers in the region, as suggested by Saaroni et al. (2010). If the current trend persists, we project additional 10 aerial exposure hours of the reef ecosystem during summer by 2050, when the hottest weather prevails. Further support for a forecast of

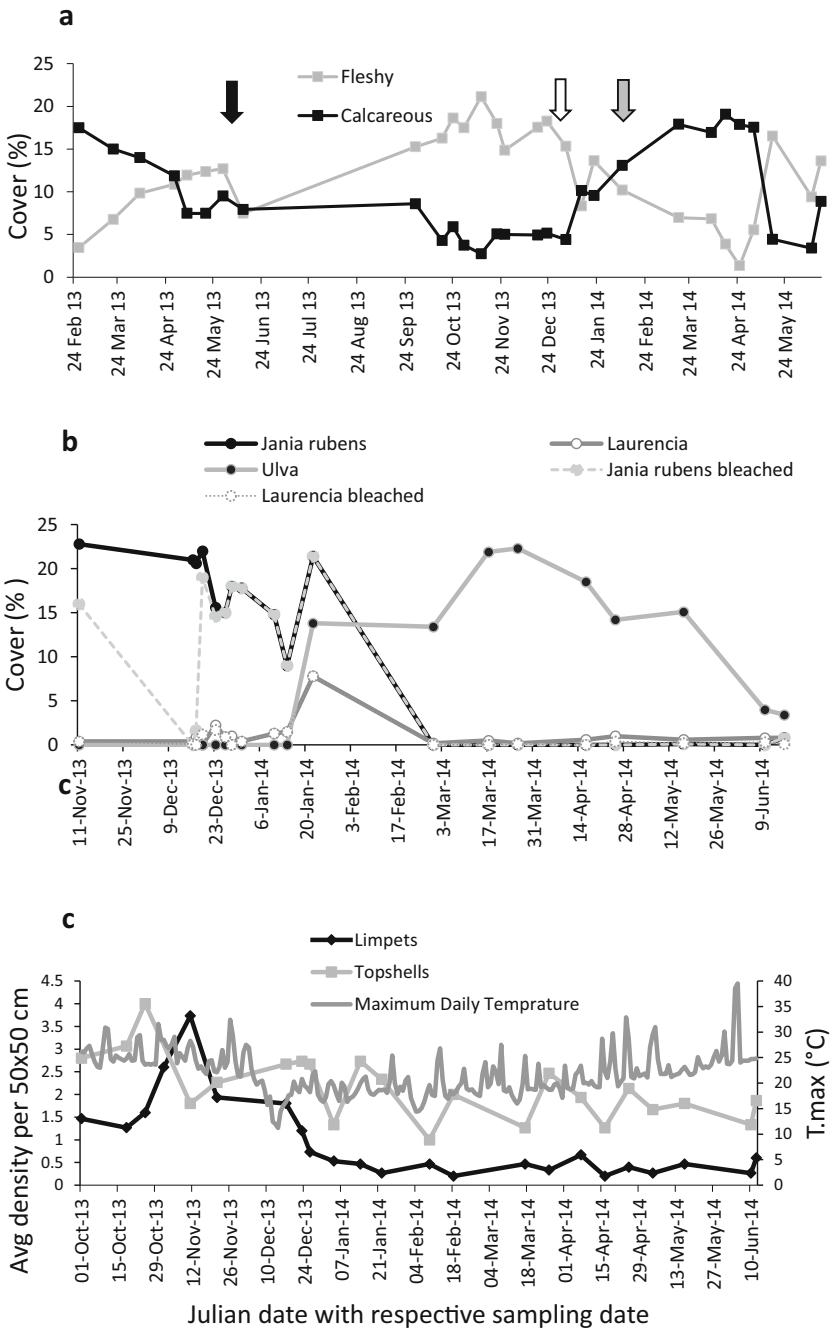

Fig. 6 Change in macroalgae functional groups at the platform edge in the random quadrats over the entire period (**a**), in cover of dominate macroalgal species (total and bleached) in the fixed quadrats during and after the main PDE of winter 2013–14 (**b**) and in the density of mobile gastropod grazers in the back reef (**c**) during the study period. Percent cover of calcareous (black) and fleshy (gray) algae at the reef edge is given for the period February 2013 and May 2014. The black arrow in **a** represents the short hot PDE indicated in Fig. 2. The white and gray arrows represent the beginning and end of a period with a series of cold, long, PDEs (indicated in Fig. 2), when the reef flat was mostly out of water and massive bleaching of all algae occurred (seen in **b**). The average density per 50 × 50-cm rock area of *Patella* (black line) and *Phorcus* (gray line) and maximum daily air temperature are shown from the end of September 2013 until mid-June 2014. The large gap in data in the summer months of 2013 (between early June and late September) is due to the difficulty to conduct ecological sampling of the platform edge during this season because of constant wave action. Observations indicate that during this season calcareous algae like *Jania rubens* are abundant on the platform

increased aerial exposure comes from a recent ensemble projection of climatic changes in synoptic system occurrences in the Eastern Mediterranean that predicts a significant increase in RST frequencies during winter and in Persian Trough frequencies by the mid- and end of the twenty-first century, on the expense of cyclone systems (Hochman et al. 2017).

Ecological Impacts of PDEs

The weekly field sampling of the community could only indicate strong impacts of extensive PDEs and not the immediate impacts of short PDEs, which will be required in future studies aimed at testing the progression of ecological impacts of different types and sequences of PDEs. The data do show a decrease in fleshy algae after exposure to the hot (in May 2013) and the cold (in December 2013) PDEs, respectively. It was impossible to follow the recovery of fleshy algae following the May hot PDE because of continuous wave action throughout the summer. Fleshy algae seemed to recover relatively quickly in late spring following the winter cold and prolonged PDE, but this "recovery" was dominated mostly by opportunistic, highly seasonal taxa, of the family Ulvacea.

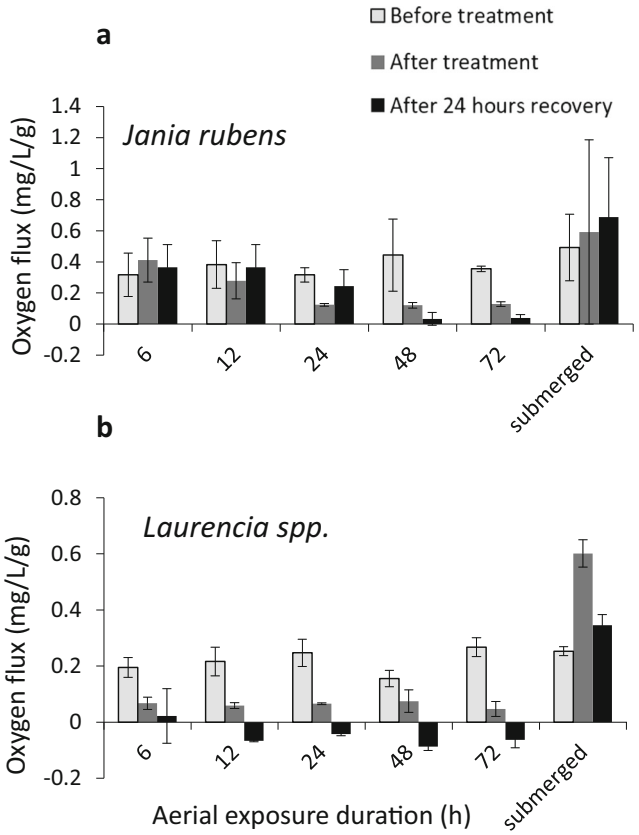

Fig. 7 Average (± SD) dissolved oxygen levels per gram algal tissue during incubation in *Jania rubens* (**a**) and *Laurencia* spp. (**b**) under different aerial exposure durations measured by incubation in water at three time steps: before the exposure, immediately after the return to water, and 24 h after the re-submergence (a recovery period) compared to individuals that were continuously submerged and measured at the same three periods

Although both functional groups are vulnerable to long desiccation stress, calcareous algae appear to be more resilient and apparently can recover faster at the population level in the field. The simple lab experiment demonstrated that the dominant representative of the low intertidal zone community in the region, *L. papillosa*, bleaches and dies within less than 6 h of aerial exposure, whereas this short exposure actually increases photosynthetic activity in the dominant intertidal calcareous algae, *J. rubens*, and it dies only after exposures longer than 24 h. The greater sensitivity of fleshy algae to aerial exposure compared to calcareous algae has been previously demonstrated (Benedetti-Cecchi et al. 2006) and is probably related to their morphological properties; however, this aspect was rarely studied and deserves further research (but see, Bell 1993, 1995). Our observations suggest that short PDEs only cause minor damage (only tips bleaching) to macroalgal mats (although they kill individual plants, as indicated by the experiment, probably because mats maintain moisture longer), which allows fast recovery (days) at the population level. We assume that slower recovery (weeks) of the algae after extreme PDEs or a sequence of PDEs, when all visible erect algal biomass is eventually removed, is possible due to the existence of a viable propagule bank in microhabitat refugia. This is because fast recruitment from distinct populations is less likely as most macroalgae propagules settle quickly and very close to the mother plant (Kinlan et al. 2005), especially in small species (Norton 1992) like those dominating Mediterranean rocky shores. We further speculate that in species where the propagule bank is also eliminated under severe PDEs, recovery will be on the order of months or even years and will depend on supply of propagules from distant source populations that were not severely affected by the PDE. The period of ecological monitoring in this study included an exceptional series of intense PDEs during the winter months, judging from 9 years of vermetid reef ecological monitoring (Rilov, unpublished data). This has both positive and negative aspects with regard to the aims of the study. On the one hand, this exceptional period demonstrated the short-term impacts of severe PDEs. On the other hand, it does not represent the ecological dynamic of the system in a "normal" year, because seasonal ecological monitoring on this coast indicates that in most winters, algal cover is high and species diversity at the edge of the platform is at its highest (Rilov in Herut 2016); while in the winter of 2013–14, the rocks were mostly covered by bleached algae which were later removed, leaving the platform with almost no macroalgae (Fig. 6a, b).

Our weekly observations revealed that topshell abundance fluctuated considerably, probably as a result of their high mobility and tendency to move into crevices and tidepools (especially during harsh conditions) where they could not be effectively counted. Topshell mortality was observed during the cold PDE of December 2013, mostly of those that were trapped in small refugia that went dry after few days of particularly strong and dry easterly winds. However, monitoring did not detect population level impacts, suggesting that this mortality had no considerable effect on the population in HaBonim. By contrast, limpets did show a considerable decrease in abundance following the cold PDE of December 2013, and limpet mortality was indeed observed, with no signs of recovery in the population for the reminder of the study period. Longer-term time-series, in multiple locations, are needed to fully understand the impacts on PDEs on this and other (mobile or sessile) animal species. Rocky intertidal topshells and especially limpets can adapt to harsh physical conditions like extreme heat, cold, or desiccation (e.g., Prusina et al. 2014; Williams and Morritt 1995), but in most regions, they experience such stress only during low tide, that is, for only a few hours. For example, the intertidal and shallow subtidal limpet on the New England coast, *Acmaea testudinalis*, did not survive beyond 48 h of desiccation conditions (Wallace 1972). This is not the case on the southeastern Mediterranean shore. Our study shows that on this coast, limpets leaving at the mid- to low shore levels can withstand many days of extreme desiccation conditions during PDEs, that can be combined with cold or very hot temperatures.

Nonetheless, the long exposure to cold, dry air did eventually lead to the death of many limpets during the winter 2013 PDE. Further research is required to determine what are the limpets tolerance limits and how do most individuals manage to survive these highly stressful desiccation conditions for extended periods, well beyond what is known for other regions. Our analysis indicates when the most potentially harmful PDEs occur. It shows that during spring, there is a strong correlation between PDE and high air temperatures as well as easterly winds (Table **2**), and the second longest PDE occurred in this season. During winter, there was a correlation between PDEs and strong easterly winds and low temperatures and the longest PDE occurred in this season.

Future Trends

We suggest that PDEs will be most ecologically harmful during spring and winter as species richness is highest during those seasons compared to summer when PDEs rarely occur and autumn when they are frequent but short, and species richness is low. In future studies, it would be interesting to compare the relative impact of cold and warm PDEs of different durations in the different seasons. Long-term monitoring of both physical and biological parameters will also help to determine the potential long-term impacts of extreme PDEs on the intertidal ecological community and local and regional biodiversity. Examining how habitat complexity can influence the provisioning of potential micro-refugia from extreme events, such as PDEs, is another important venue of research.

In conclusion, the unique and fragile biogenic vermetid reef ecosystem that has already suffered from the loss of its main reef builder, *D. petraeum*, and one of its main predators, the whelk *Stramonita haemastoma* (Rilov 2016), is evidently experiencing increased desiccation stress with the apparent increase in the frequency of PDE-generating synoptic systems. Further research is needed to explore the PDE phenomenon and its ecological impacts in the context of climate change. For example, it has been shown that different dynamics of the variance in aerial exposure can have different effects on low shore ecological communities in the western Mediterranean, where PDEs were not reported (Benedetti-Cecchi et al. 2006). The importance of the dynamics (frequency, intervals, intensity) of PDE extreme events deserves special attention in future PDE studies. We provided very basic, back-of-the-envelope, projections of the potential increase of aerial exposure hours on the reef by 2050. These forecasts do not take into account the climate change-driven rising of sea level, which appears to be much higher than the global average on the Israeli coast (about 13 cm since 1992, see Rosen et al. 2013). It is possible that sea level rise might counter the occurrence or intensity of PDEs and thus ameliorate their ecological impacts on the rocky shore. In the coming decades, it will be imperative to study the relative importance of these two, perhaps contrasting, facets of global change to the integrity of coastal ecological communities.

Acknowledgments We thank T. Guy-Haim for assistance in the design and analysis of the experiments and L. Sever, E. Ilotoviz, E. Yeruham, and O. Rave in data collection and analysis. This article is dedicated to the memory of Dr. Rana Samuels, an extraordinary climate researcher who helped with the climate data analysis and the initial design of the study.

Funding Information This research was supported in part by the Smaller-Winnikow Scholarship Fund in cooperation with the Keren Kayemet L'Israel (Jewish National Fund—JNF) (to RZ), the Porter School for Environmental Studies, the Israel Science Foundation, grant number 1217/10 (to GR), the Marie Curie Reintegration Programme under the EU Seventh Framework, grant number 249147 (to GR), and the Ministry of Environmental Protection (supporting IOLR National Monitoring Program).

References

Alpert, P., T. Ben-Gai, A. Baharad, Y. Benjamini, D. Yekutieli, M. Colacino, L. Diodato, C. Ramis, V. Homar, and R. Romero. 2002. The paradoxical increase of Mediterranean extreme daily rainfall in spite of decrease in total values. *Geophysical Research Letters* 29 (11).

Alpert, P., I. Osetinsky, B. Ziv, and H. Shafir. 2004. Semi-objective classification for daily synoptic systems: application to the eastern Mediterranean climate change. *International Journal of Climatology* 24 (8): 1001–1011.

Alpert, P., S.O. Krichak, H. Shafir, D. Haim, and I. Osetinsky. 2008. Climatic trends to extremes employing regional modeling and statistical interpretation over the E. Mediterranean. *Global and Planetary Change* 63 (2-3): 163–170.

Bell, E. 1993. Photosynthetic response to temperature and desiccation of the intertidal alga *Mastocarpus papillatus*. *Marine Biology* 117 (2): 337–346.

Bell, E.C. 1995. Environmental and morphological influences on thallus temperature and desiccation of the intertidal alga *Mastocarpus papillatus* Kützing. *Journal of Experimental Marine Biology and Ecology* 191 (1): 29–55.

Benedetti-Cecchi, L., I. Bertocci, S. Vaselli, and E. Maggi. 2006. Temporal variance reverses the impact of high mean intensity of stress in climate change experiments. *Ecology* 87 (10): 2489–2499.

Chemello, R., and S. Silenzi. 2011. Vermetid reefs in the Mediterranean Sea as archives of sea-level and surface temperature changes. *Chemistry & Ecology* 27 (2): 121–127.

Council, A. 2001. Statement on seasonal to interannual climate prediction. *Bulletin of the American Meteorological Society* 82: 701.

Diffenbaugh, N.S., and C.B. Field. 2013. Changes in ecologically critical terrestrial climate conditions. *Science* 341 (6145): 486–492.

Dong, Y., L.P. Miller, J.G. Sanders, and G.N. Somero. 2008. Heat-shock protein 70 (Hsp70) expression in four limpets of the genus *Lottia*: interspecific variation in constitutive and inducible synthesis correlates with in situ exposure to heat stress. *The Biological Bulletin* 215 (2): 173–181.

Evans, J.P. 2009. 21st century climate change in the Middle East. *Climatic Change* 92 (3-4): 417–432.

Garrabou, J., R. Coma, N. Bensoussan, M. Bally, P. Chevaldonne, M. Cigliano, D. Diaz, J.G. Harmelin, M.C. Gambi, D.K. Kersting, J.B. Ledoux, C. Lejeusne, C. Linares, C. Marschal, T. Perez, M. Ribes, J.C. Romano, E. Serrano, N. Teixido, O. Torrents, M. Zabala, F. Zuberer, and C. Cerrano. 2009. Mass mortality in Northwestern

Mediterranean rocky benthic communities: effects of the 2003 heat wave. *Global Change Biology* 15 (5): 1090–1103.

Gattuso, J.-P., A. Magnan, R. Billé, W. Cheung, E. Howes, F. Joos, D. Allemand, L. Bopp, S. Cooley, and C. Eakin. 2015. Contrasting futures for ocean and society from different anthropogenic CO_2 emissions scenarios. *Science* 349 (6243): aac4722.

Grange, S. K. 2014. *Technical note: averaging wind speeds and directions*. [Technical report] doi:https://doi.org/10.13140/RG.2.1.3349.2006.

Harley, C.D.G., and B.S.T. Helmuth. 2003. Local- and regional-scale effects of wave exposure, thermal stress, and absolute versus effective shore level on patterns of intertidal zonation. *Limnology and Oceanography* 48 (4): 1498–1508.

Harley, C.D.G., A.R. Hughes, K.M. Hultgren, B.G. Miner, C.J.B. Sorte, C.S. Thornber, L.F. Rodriguez, L. Tomanek, and S.L. Williams. 2006. The impacts of climate change in coastal marine systems. *Ecology Letters* 9 (2): 228–241.

Harley, C.D., S.D. Connell, Z.A. Doubleday, B. Kelaher, B.D. Russell, G. Sarà, and B. Helmuth. 2017. Conceptualizing ecosystem tipping points within a physiological framework. *Ecology and Evolution.* 7 (15): 6035–6045.

Helmuth, B., C.D.G. Harley, P.M. Halpin, M. O'Donnell, G.E. Hofmann, and C.A. Blanchette. 2002. Climate change and latitudinal patterns of intertidal thermal stress. *Science* 298 (5595): 1015–1017.

Helmuth, B., N. Mieszkowska, P. Moore, and S.J. Hawkins. 2006. Living on the edge of two changing worlds: forecasting the responses of rocky intertidal ecosystems to climate change. *Annual Review of Ecology Evolution and Systematics* 37 (1): 373–404.

Helmuth, B., B.D. Russell, S.D. Connell, Y. Dong, C.D. Harley, F.P. Lima, G. Sará, G.A. Williams, and N. Mieszkowska. 2014. Beyond long-term averages: making biological sense of a rapidly changing world. *Climate Change Responses* 1 (1).

Herut, B. 2016. *The national monitoring program of Israel's Mediterranean waters—scientific report for 2015, IOLR, Report H42/2016: National Institute of Oceanography, Israel Oceanographic and Limnological Research.*

Hochman, A., T. Harpaz, H. Saaroni, and P. Alpert. 2017. Synoptic classification in 21st century CMIP5 predictions over the Eastern Mediterranean with focus on cyclones. *International Journal of Climatology.*

IPCC. 2012. Managing the risks of extreme events and disasters to advance climate change adaptation. *A special report of Working Groups I and II of the Intergovernmental Panel on Climate Change*, ed. C.B. Field, V. Barros, T.F. Stocker, D. Qin, D.J. Dokken, K.L. Ebi, M.D. Mastrandrea, K.J. Mach, G.-K. Plattner, S.K. Allen, M. Tignor, and P.M. Midgley (eds). 582 Cambridge, UK, and New York, NY, USA.

IPCC. 2013. *Climate change 2013: the physical science basis. Contribution of Working Group I to the Fifth Assessment Report of the Intergovernmental Panel on Climate Change*. Cambridge, United Kingdom and New York, NY, USA: Cambridge University Press.

Jonsson, P.R., L. Granhag, P.S. Moschella, P. Åberg, S.J. Hawkins, and R.C. Thompson. 2006. Interactions between wave action and grazing control the distribution of intertidal macroalgae. *Ecology* 87 (5): 1169–1178.

Kelley, C.P., S. Mohtadi, M.A. Cane, R. Seager, and Y. Kushnir. 2015. Climate change in the Fertile Crescent and implications of the recent Syrian drought. *Proceedings of the National Academy of Sciences* 112 (11): 3241–3246.

Kinlan, B.P., S.D. Gaines, and S.E. Lester. 2005. Propagule dispersal and the scales of marine community process. *Diversity and Distributions* 11 (2): 139–148.

Kitoh, A., A. Yatagai, and P. Alpert. 2008. First super-high-resolution model projection that the ancient "Fertile Crescent" will disappear in this century. *Hydrological Research Letters* 2: 1–4.

Kostopoulou, E., C. Giannakopoulos, M. Hatzaki, A. Karali, P. Hadjinicolaou, J. Lelieveld, and M. Lange. 2013. Assessment of climate change extremes over the Eastern Mediterranean and Middle East region using the Hadley Centre PRECIS Regional Climate Model. In *Advances in meteorology, climatology and atmospheric physics*, 547–554. Springer.

Lejeusne, C., P. Chevaldonné, C. Pergent-Martini, C.F. Boudouresque, and T. Pérez. 2010. Climate change effects on a miniature ocean: the highly diverse, highly impacted Mediterranean Sea. *Trends in Ecology & Evolution* 25 (4): 250–260.

Lelieveld, J., P. Hadjinicolaou, E. Kostopoulou, J. Chenoweth, M. El Maayar, C. Giannakopoulos, C. Hannides, M. Lange, M. Tanarhte, and E. Tyrlis. 2012. Climate change and impacts in the Eastern Mediterranean and the Middle East. *Climatic Change* 114 (3-4): 667–687.

Lesk, C., P. Rowhani, and N. Ramankutty. 2016. Influence of extreme weather disasters on global crop production. *Nature* 529 (7584): 84–87.

Lipkin, Y., and U. Safriel. 1971. Intertidal zonation of the rocky shores at Mikhmoret (Mediterranean, Israel). *Journal of Ecology* 59 (1): 1–30.

Mann, M.E., and P.H. Gleick. 2015. Climate change and California drought in the 21st century. *Proceedings of the National Academy of Sciences* 112 (13): 3858–3859.

Marbà, N., G. Jorda, S. Agusti, C. Girard, and C.M. Duarte. 2015. Footprints of climate change on Mediterranean Sea biota. *Frontiers in Marine Science* 2.

Martone, P.T., M. Alyono, and S. Stites. 2010. Bleaching of an intertidal coralline alga: untangling the effects of light, temperature, and desiccation. *Marine Ecology Progress Series* 416: 57–67.

Mislan, K.A.S., C.A. Blanchette, B.R. Broitman, and L. Washburn. 2011. Spatial variability of emergence, splash, surge, and submergence in wave-exposed rocky-shore ecosystems. *Limnology and Oceanography* 56 (3): 857–866.

Molinos, J.G., B.S. Halpern, D.S. Schoeman, C.J. Brown, W. Kiessling, P.J. Moore, J.M. Pandolfi, E.S. Poloczanska, A.J. Richardson, and M.T. Burrows. 2015. Climate velocity and the future global redistribution of marine biodiversity. *Nature Climate Change.*

Montes-Hugo, M., S.C. Doney, H.W. Ducklow, W. Fraser, D. Martinson, S.E. Stammerjohn, and O. Schofield. 2009. Recent changes in phytoplankton communities associated with rapid regional climate change along the western Antarctic Peninsula. *Science* 323 (5920): 1470–1473.

Norton, T. 1992. Dispersal by macroalgae. *British Phycological Journal* 27 (3): 293–301.

Osetinsky, I. 2006. *Climate changes over the E. Mediterranean—a synoptic systems classification approach*. Tel Aviv: University Tel Aviv University.

Ozer, T., I. Gertman, N. Kress, J. Silverman, and B. Herut. 2016. *Interannual thermohaline (1979–2014) and nutrient (2002–2014) dynamics in the Levantine surface and intermediate water masses*. Global and Planetary Change: SE Mediterranean Sea.

Pala, C. 2016. Corals tie stronger El Niños to climate change: American Association for the Advancement of Science.

Parmesan, C., and G. Yohe. 2003. A globally coherent fingerprint of climate change impacts across natural systems. *Nature* 421 (6918): 37–42.

Petes, L.E., B.A. Menge, and G.D. Murphy. 2007. Environmental stress decreases survival, growth, and reproduction in New Zealand mussels. *Journal of Experimental Marine Biology and Ecology* 351 (1-2): 83–91.

Prendergast, A., M. Azzopardi, T. O'Connell, C. Hunt, G. Barker, and R. Stevens. 2013. Oxygen isotopes from *Phorcus* (*Osilinus*) *turbinatus* shells as a proxy for sea surface temperature in the central Mediterranean: a case study from Malta. *Chemical Geology* 345: 77–86.

Prusina, I., G. Sarà, M. De Pirro, Y.-W. Dong, G.-D. Han, B. Glamuzina, and G.A. Williams. 2014. Variations in physiological responses to thermal stress in congeneric limpets in the Mediterranean Sea. *Journal of Experimental Marine Biology and Ecology* 456: 34–40.

Rilov, G. 2016. Multi-species collapses at the warm edge of a warming sea. *Scientific Reports* 6 (1).

Rilov, G., Y. Benayahu, and A. Gasith. 2004. Prolonged lag in population outbreak of an invasive mussel: a shifting-habitat model. *Biological Invasions* 6 (3): 347–364.

Rivetti, I., S. Fraschetti, P. Lionello, E. Zambianchi, and F. Boero. 2014. Global warming and mass mortalities of benthic invertebrates in the Mediterranean Sea. *PLoS One* 9 (12): e115655.

Romm, J. 2011. Desertification: The next dust bowl. *Nature* 478 (7370): 450–451.

Rosen, S.D., L. Raskin, and B. Galanti. 2013. Long-term characteristics of sea level, wave, wind and current at central Mediterranean coast of Israel from 20 years of data at GLOSS station 80—Hadera. In *40th CIESM Congress*. Marseille.

Saaroni, H., B. Ziv, A. Bitan, and P. Alpert. 1998. Easterly wind storms over Israel. *Theoretical and Applied Climatology* 59 (1-2): 61–77.

Saaroni, H., B. Ziv, I. Osetinsky, and P. Alpert. 2010. Factors governing the interannual variation and the long-term trend of the 850 hPa temperature over Israel. *Quarterly Journal of the Royal Meteorological Society* 136: 305–318.

Safriel, U.N. 1974. Vermetid gastropods and intertidal reefs in Israel and Bermuda. *Science* 186 (4169): 1113–1115.

Safriel, U.N. 1975. The role of vermetid gastropods in the formation of Mediterranean and Atlantic reefs. *Oecologia (Berlin)* 20 (1): 85–101.

Shentsis, I., J.B. Laronne, and P. Alpert. 2012. Red Sea Trough flood events in the Negev, Israel (1964–2007). *Hydrological Sciences Journal* 57 (1): 42–51.

Sisma-Ventura, G., R. Yam, and A. Shemesh. 2014. Recent unprecedented warming and oligotrophy of the eastern Mediterranean Sea within the last millennium. *Geophysical Research Letters* 41 (14): 5158–5166.

Sydeman, W., M. García-Reyes, D. Schoeman, R. Rykaczewski, S. Thompson, B. Black, and S. Bograd. 2014. Climate change and wind intensification in coastal upwelling ecosystems. *Science* 345 (6192): 77–80.

Tielbörger, K., M.C. Bilton, J. Metz, J. Kigel, C. Holzapfel, E. Lebrija-Trejos, I. Konsens, H.A. Parag, and M. Sternberg. 2014. Middle-eastern plant communities tolerate 9 years of drought in a multi-site climate manipulation experiment. *Nature Communications* 5: 5102.

Ummenhofer, C.C., and G.A. Meehl. 2017. Extreme weather and climate events with ecological relevance: a review. *The royal society B* 372: 20160135.

Vasseur, D.A., J.P. DeLong, B. Gilbert, H.S. Greig, C.D. Harley, K.S. McCann, V. Savage, T.D. Tunney, and M.I. O'Connor. 2014. Increased temperature variation poses a greater risk to species than climate warming. *Proceedings of the Royal Society B: Biological Sciences* 281 (1779): 20132612.

Visser, M.E., and C. Both. 2005. Shifts in phenology due to global climate change: the need for a yardstick. *Proceedings of the Royal Society of London B: Biological Sciences* 272 (1581): 2561–2569.

Wallace, L.R. 1972. Some factors affecting vertical distribution and resistance to desiccation in the limpet, *Acmaea testudinalis* (Muller). *The Biological Bulletin* 142 (1): 186–193.

Wernberg, T., S. Bennett, R.C. Babcock, T. de Bettignies, K. Cure, M. Depczynski, F. Dufois, J. Fromont, C.J. Fulton, R.K. Hovey, E.S. Harvey, T.H. Holmes, G.A. Kendrick, B. Radford, J. Santana-Garcon, B.J. Saunders, D.A. Smale, M.S. Thomsen, C.A. Tuckett, F. Tuya, M.A. Vanderklift, and S. Wilson. 2016. Climate-driven regime shift of a temperate marine ecosystem. *Science* 353 (6295): 169–172.

Williams, G.A., and D. Morritt. 1995. Habitat partitioning and thermal tolerance in a tropical limpet, *Cellana grata*. *Marine Ecology Progress Series* 124: 89–103.

Williams, G.A., C. Little, D. Morritt, P. Stirling, L. Teagle, A. Miles, G. Pilling, and M. Consalvey. 1999. Foraging in the limpet *Patella vulgata*: the influence of rock slope on the timing of activity. *Journal of the Marine Biological Association of the UK* 79 (5): 881–890.

Yeruham, E., G. Rilov, M. Shpigel, and A. Abelson. 2015. Collapse of the echinoid *Paracentrotus lividus* populations in the Eastern Mediterranean—result of climate change? *Scientific Reports* 5 (1): 13479.

Zhang, X., E. Aguilar, S. Sensoy, H. Melkonyan, U. Tagiyeva, N. Ahmed, N. Kutaladze, F. Rahimzadeh, A. Taghipour, and T. Hantosh. 2005. Trends in Middle East climate extreme indices from 1950 to 2003. *Journal of Geophysical Research: Atmospheres* 110 (D22).